



Computational investigation of dioxin-like compounds as human sex hormone-binding globulin inhibitors: DFT calculations, docking study and molecular dynamics simulations

Nikita Tiwari, Ashutosh Kumar, Anjali Pandey, Anil Mishra *

Department of Chemistry, University of Lucknow, Lucknow 226007, India

ARTICLE INFO

Edited by Dr. Mark Cronin

Keywords:

DLCs
DFT
Docking
GROMACS
Sex hormone-binding globulin

ABSTRACT

Polychlorinated dibenzo-p-dioxins/dibenzofurans (PCDD/Fs) and polychlorinated biphenyls (PCBs) are omnipresent and persistent environmental pollutants. In particular, 29 congeners are of special concern, and these are usually referred to as dioxin-like compounds (DLCs). Sex hormone binding globulin (SHBG) is a circulatory protein that binds sex steroids and is a potential target for endocrine disruptors in the human body. Herein, we report the optimization of DLCs employing density functional theory (DFT) to elucidate their frontier molecular orbitals and also the reactivity descriptors. The DFT outcome revealed that PCDFs and PCBs show the high dipole moment as well as high electrophilicity index and basicity. To assess the structure based inhibitory action of DLCs, these were docked into the active site cavity of hSHBG. Docking results show that the binding affinities of DLCs lie in the comparable range (-7.19 kcal/mol to -9.12 kcal/mol) with Dihydrotestosterone (-10.94 kcal/mol), a substrate analogue of hSHBG. DLCs interact with the key residues such as Ser42, Asp65 and Asn82 and lie within the active site of hSHBG. Dynamics and stability of the DLCs-hACMSD complexes were determined by performing molecular dynamics simulations using GROMACS 5.1.1. The results emphasize that DLCs can structurally mimic the binding pattern of DHT to hSHBG, which further leads to inhibition of its activity.

1. Introduction

Pollution is known to impact the environment and affect humans and animals by triggering various mechanisms of toxicity [1]. Well-documented examples at the molecular level are the binding of heavy metals to enzymes [2], the binding of polycyclic aromatic hydrocarbons to DNA [3], hormonal disturbance by dioxins and polychlorinated biphenyls (PCBs), and other effects, like reproductive disorders due to phthalates. All of these mechanisms have one thing in common: By displacing natural compounds, pollutants block and modify physiological processes and pathways and induce genotoxicity, mutagenicity, and also carcinogenicity. Chemically reactive metabolites or pollutants can also lead to conformational changes that affect the function of proteins [4,5], which alter and reduce their biological function. Chemicals capable of interfering with the functions of endocrine systems are referred to as endocrine-disrupting chemicals (EDCs). The National Resources Defense Council (1998) defined an endocrine disruptor as a compound, which when absorbed into the body, acts as either an agonist or antagonist of hormone action and disrupts the body's normal balance.

The toxicological effects of polychlorinated biphenyls (PCBs) and Polychlorinated dibenzo-p-dioxins/dibenzofurans (PCDD/Fs) are diverse, ranging from chloracne and immunological effects in humans to severe weight loss, thymic atrophy, hepatotoxicity, immunotoxicity, endocrine disruption, and carcinogenesis in rodents [6]. PCDD/Fs and PCBs are examples of persistent organic pollutants. PCDD/Fs have no practical use in society, but are produced as by-products in, for example, combustion processes, while PCBs were used in the past for things like electronic insulators and sealants in building construction. PCDD/Fs and PCBs are halogenated aromatic compounds, including a large range of congeners. These congeners differ from each other by the number of chlorine atoms substituted on the aromatic rings and their substitution pattern on the rings (Fig. 1).

Out of the theoretically possible 75 PCDDs, 135 PCDFs, and 209 PCBs, 29 congeners are referred to as DLCs. These twenty-nine dioxin-like PCBs and PCDD/Fs have been assigned toxic equivalency factors (TEFs) in Table 1 [7]. The TEF concept was developed during the 1980s as a method for risk assessment of PCDD/Fs [8]. Today, TEFs provide a unique tool for assessing the toxic potency of mixtures of DLCs in food,

* Corresponding author.

E-mail addresses: mishraanil101@hotmail.com, nikitalko23@gmail.com (A. Mishra).

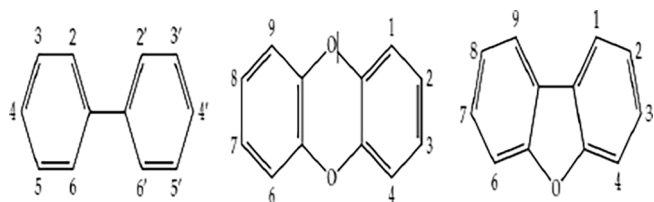


Fig. 1. The general structural formulas and substitution positions of (left to right) polychlorinated biphenyls (PCBs), dibenzo-p-dioxins (PCDDs), and dibenzofurans (PCDFs).

feed, human populations, and wildlife [9]. Each DLC is assigned a relative value that relates the DLC's potency to the potency of 2378-TCDD. A congener with a TEF value of 0.1 means that ten times as much of that DLC is needed to induce the same effect as 2378-TCDD. Due to their high hydrophobicity, DLCs primarily partition to organic matter in soil and sediment and they accumulate in adipose tissues of organisms. DLCs bioaccumulate, and as a result they are found at high concentrations in top-level predators in the food chains, such as eagles, seals, and humans. Moreover, DLCs have been shown to have various negative impacts on organisms [10].

The recent trend towards reducing and replacing animal testing has led to several *in vitro* and *in silico* methods for studying toxicity [11]. These studies give quick and accurate results and can even be carried out virtually on hypothetical chemicals. In recent years, a novel screening method involving *in silico* DFT and docking calculations are used to identify toxic chemicals and EDCs [12]. Endocrine disruptors are chemicals that target the human nuclear receptor and bind with active sites of the receptors known as the ligand-binding domain (LBD). Molecular docking studies facilitate the prediction of a possible molecular interaction of toxic ligands with enzymes of various pathways leading to the production of vital molecules and elucidate subsequent molecular cross-talk within the system [13]. Researchers used the *in silico* approach to establish the endocrine disrupting action of the alternative plasticizers, the chemicals used in making surgical equipment and toys.

In silico approaches were used to reveal interactions of environmental xenoestrogens with human SHBG [14]. However, no docking analysis of DLCs with human SHBG are available to date.

It has been proposed that "EDCs exert their toxic effects through interactions with nuclear steroid receptors, sex steroid-binding proteins and enzymatic pathways regulating the reproductive and endocrine functions" [15]. SHBG is a circulating and plasma carrier protein. It binds with sex steroids and plays a vital role in maintaining the balance between unbound and bound sex hormones [16]. Any changes in SHBG level affects the distribution of the sex steroids to target tissues. SHBG has also been reported to bind with several EDCs such as phthalate esters [17]. Binding of several EDCs with zebrafish homolog of SHBG has been reported [18]. Recently molecular modelling of many plasticizers with sex hormone receptors has been reported [19].

There is no experimental evidence reported so far that can clearly prove that DLCs binds to human SHBG. However, there is some indirect evidence that shows the possibility of such binding. DLCs have many documented adverse health effects. They have been linked to cancer, heart disease, hormonal problems, asthma, cognitive problems, suppression of the immune system, and IQ deficits in infants [20]. Sex hormone-binding globulin (SHBG) was found to be positively associated with both prenatal and concurrent PCB exposures [21]. As the indirect evidence is suggestive of a possible binding between the DLCs and human SHBG, the present *in silico* study is undertaken to verify whether such a binding is energetically possible.

The objective of current study involved computational approaches to understand the mechanism of molecular interaction of DLCs with human SHBG using DFT calculations, molecular docking and simulation studies. The details of the binding mechanism of these compounds were analyzed individually and then comparisons of the distinctive binding pattern of these with dihydrotestosterone (DHT) were performed. In view of the reported deleterious effects of DLCs on human reproduction, the present study is an innovative step and may further help in understanding the interfering mechanism and its undesirable effects on human reproductive health.

Table 1

Calculated electronegativity (χ), global hardness (η), softness (δ), global electrophilicity index (ω) of investigated ligands.

DLCs/Ligand category	DLC/ Ligand	HOMO	LUMO	ΔE	η	χ	δ	ω	
Inhibitor	DHT	-6.14	-0.17	5.97	2.98	3.15	0.33	1.66	
Chlorinated dibenzo-p-dioxins	2,3,7,8-TCDD	-6.33	-1.50	4.83	2.41	3.91	0.41	3.17	
	1,2,3,7,8-PeCDD	-6.49	-1.73	4.76	2.38	4.11	0.42	3.54	
	1,2,3,4,7,8-HxCDD	-6.64	-2.17	4.47	2.23	4.40	0.44	4.34	
	1,2,3,6,7,8-HxCDD	-6.65	-1.90	4.75	2.37	4.27	0.42	3.84	
	1,2,3,7,8,9-HxCDD	-6.64	-1.88	4.76	2.38	4.26	0.42	3.81	
	1,2,3,4,6,7,8-HpCDD	-6.79	-2.25	4.54	2.27	4.52	0.44	4.50	
	OCDD	-6.93	-2.40	4.53	2.26	4.66	0.44	4.80	
	Chlorinated dibenzofurans	2,3,7,8-TCDF	-7.02	-2.09	4.93	2.46	4.55	0.40	4.20
		1,2,3,7,8-PeCDF	-7.18	-2.27	4.91	2.45	4.72	0.40	4.54
		2,3,4,7,8-PeCDF	-7.13	-2.24	4.89	2.44	4.68	0.40	4.48
1,2,3,4,7,8-HxCDF		-7.25	-2.41	4.84	2.42	4.83	0.41	4.82	
1,2,3,6,7,8-HxCDF		-7.30	-2.41	4.89	2.44	4.85	0.40	4.82	
1,2,3,7,8,9-HxCDF		-7.33	-2.43	4.90	2.45	4.88	0.40	4.86	
2,3,4,6,7,8-HxCDF		-7.27	-2.41	4.86	2.43	4.84	0.41	4.82	
1,2,3,4,6,7,8-HpCDF		-7.35	-2.57	4.78	2.39	4.96	0.41	5.14	
1,2,3,4,7,8,9-HpCDF		-7.39	-2.56	4.83	2.41	4.97	0.41	5.12	
OCDF		-7.44	-2.72	4.72	2.36	5.08	0.42	5.46	
Non-ortho-substituted PCBs	3,3',4,4'-tetraCB	-7.02	-1.74	5.28	2.64	4.38	0.37	3.63	
	3,4,4',5-tetraCB	-6.87	-2.00	4.87	2.43	4.43	0.41	4.03	
	3,3',4,4',5-pentaCB	-7.21	-1.96	5.25	2.62	4.58	0.38	4.00	
	3,3',4,4',5,5'-hexaCB	-7.26	-2.44	4.82	2.41	4.85	0.41	4.88	
	Mono-ortho-substituted PCBs	2,3,3',4,4'-pentaCB	-7.23	-1.72	5.51	2.75	4.47	0.36	3.63
2,3,4,4',5-pentaCB		-7.17	-1.88	5.29	2.64	4.52	0.37	3.86	
2,3',4,4',5-pentaCB		-7.23	-1.83	5.40	2.70	4.53	0.37	3.80	
2',3,4,4',5-pentaCB		-7.27	-1.80	5.47	2.73	4.53	0.36	3.75	
2,3,3',4,4',5-hexaCB		-7.19	-2.41	4.78	2.39	4.80	0.41	4.82	
2,3,3',4,4',5'-hexaCB		-7.41	-1.93	5.48	2.74	4.67	0.36	3.97	
2,3',4,4',5,5'-hexaCB		-7.40	-2.04	5.36	2.68	4.72	0.37	4.15	
2,3,3',4,4',5,5'-heptaCB		-7.56	-2.12	5.44	2.72	4.84	0.36	4.30	

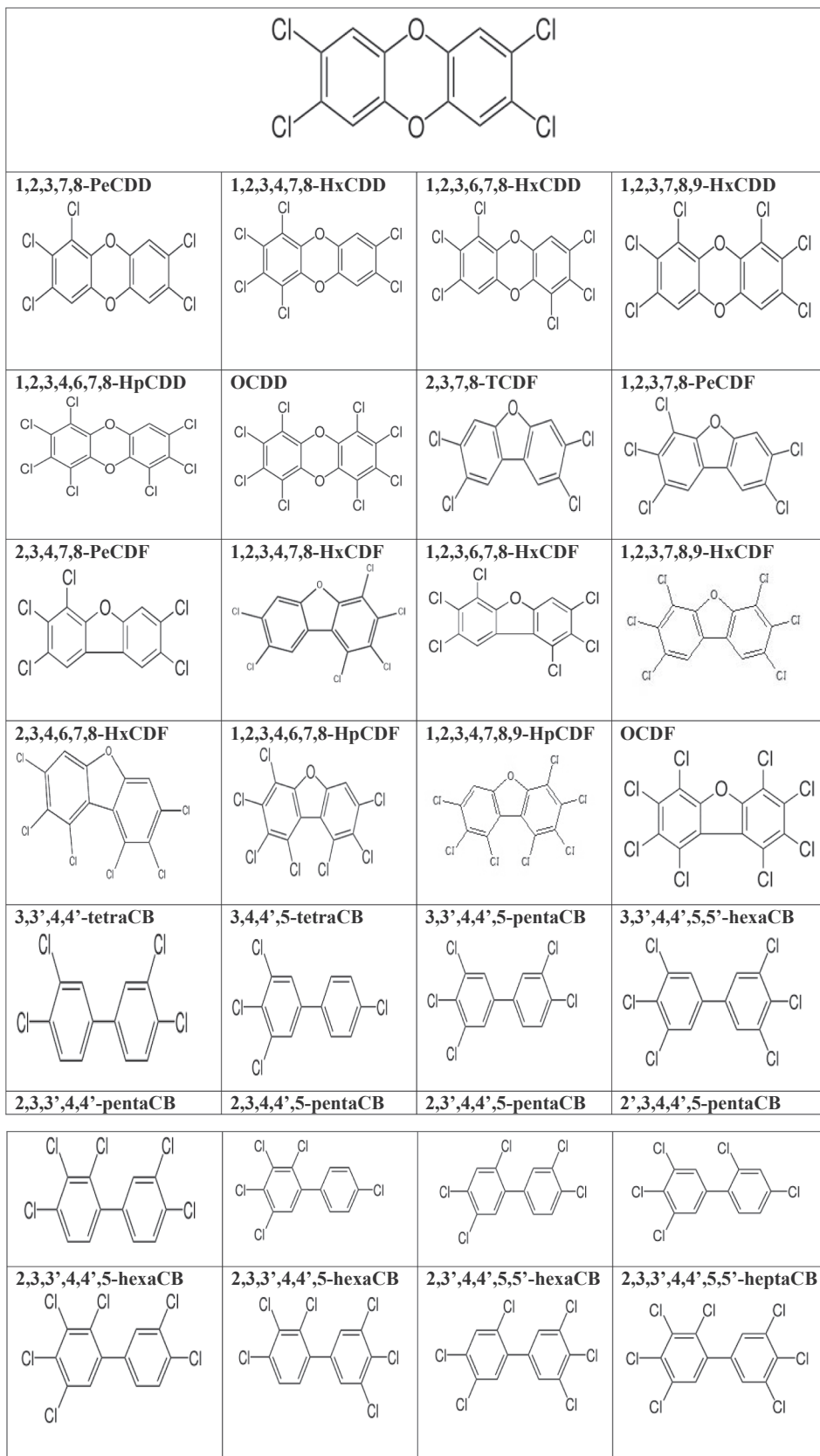


Fig. 2. The two-dimensional structure of the dioxin-like compounds.

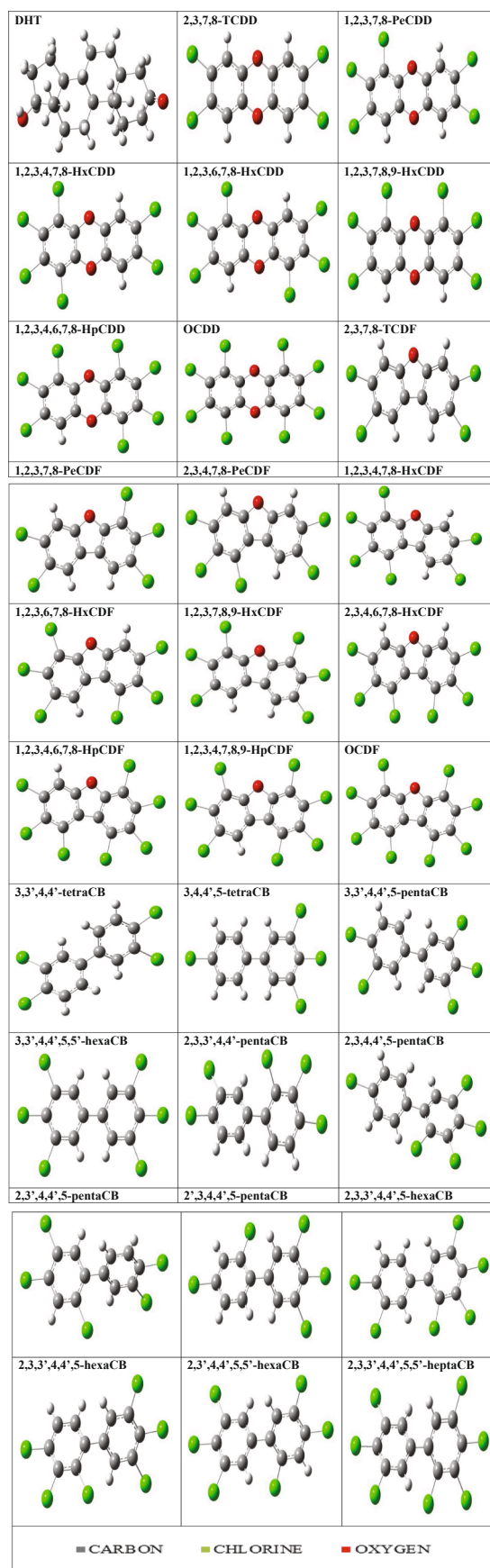


Fig. 3. Three dimensional representation of investigated DLCs and known inhibitor, DHT.

2. Materials and methods

The dioxin-like compounds taken for investigation includes 7 polychlorinated dibenzo-p-dioxins, 10 polychlorinated dibenzofurans, 4 non-*ortho*-substituted polychlorinated biphenyls and 8 mono-*ortho*-substituted polychlorinated biphenyls. Here, polychlorinated dibenzo-p-dioxins (PCDDs) are 2,3,7,8-tetrachlorodibenzo-p-dioxin (TCDD); 1,2,3,7,8-pentachlorodibenzo-p-dioxin (PeCDD); 1,2,3,4,7,8-hexachlorodibenzo-p-dioxin (HxCDD); 1,2,3,6,7,8-hexachlorodibenzo-p-dioxin (HxCDD); 1,2,3,7,8,9-hexachlorodibenzo-p-dioxin (HxCDD); 1,2,3,4,6,7,8-heptachlorodibenzo-p-dioxin (HpCDD) and octachlorodibenzo-p-dioxin (OCDD). Polychlorinated dibenzofurans (PCDFs) are 2,3,7,8-tetrachlorodibenzofuran (TCDF); 1,2,3,7,8-pentachlorodibenzofuran (PeCDF); 2,3,4,7,8-pentachloro dibenzofuran (PeCDF); 1,2,3,4,7,8-hexachlorodibenzofuran (HxCDF); 1,2,3,7,8,9-hexachlorodibenzofuran (HxCDF); 2,3,4,6,7,8-hexachlorodibenzofuran (HxCDF); 1,2,3,4,6,7,8-heptachlorodibenzofuran (HpCDF); 1,2,3,4,7,8,9-heptachlorodibenzofuran (HpCDF) and octachlorodibenzofuran (OCDF). Non-*ortho*-substituted polychlorinated biphenyls (PCBs): 3,3',4,4'-tetrachlorobiphenyl (tetraCB); 3,4,4',5'-tetrachlorobiphenyl (tetraCB); 3,3',4,4',5'-pentachlorobiphenyl (pentaCB) and 3,3',4,4',5,5'-hexachlorobiphenyl (hexaCB). Mono-*ortho*-substituted polychlorinated biphenyls (PCBs): 2,3,3',4,4'-pentachlorobiphenyl (pentaCB); 2,3,4,4',5'-pentachlorobiphenyl (pentaCB); 2',3,4,4',5'-pentachlorobiphenyl (pentaCB); 2,3,3',4,4',5'-hexachlorobiphenyl (hexaCB); 2,3,3',4,4',5'-hexachlorobiphenyl (hexaCB); 2,3',4,4',5,5'-hexachlorobiphenyl (hexaCB) and 2,3,3',4,4',5,5'-heptachlorobiphenyl (heptaCB). The two-dimensional structure of the dioxin-like compounds has been extracted from PubChem, shown in Fig. 2.

2.1. DFT calculations

Quantum mechanical (QM) methods keep an important role for the calculation of thermal and molecular orbital properties [22]. In this investigation, QM calculation was implemented by using density functional theory (DFT) employing Becke's (B) [23] exchange functional combining Lee, Yang and Parr's (LYP) correlation functional [24] in Gaussian 09 program package for all compounds [25]. People's 3-21G basis set was used to optimize the DLCs and other calculations [26]. The structural geometry was optimized by minimizing its energies compared to all geometrical variables without forcing any molecular symmetry restrictions. The molecular structure of the optimized ligands has been drawn by GaussView 5.0. [27], shown in Fig. 3. The theoretical DFT calculations were performed with Gaussian09 software at B3LYP 3-21G basis set. For every molecule's free energy and dipole moment were calculated. Frontier molecular orbital calculation was performed by using same level of theory. Hardness (η) and softness of all ligands were also calculated from the energies of frontier HOMOs and LUMOs considering Parr and Pearson interpretation [28,29] of DFT and Koopmans theorem [30] on the correlation of ionization potential (I) and electron affinities (E) with HOMO and LUMO energy (ϵ). The following equations are used for the calculation of hardness (η), electronegativity (χ) and softness (δ):

$$\eta = -1/2(E_{\text{HOMO}} - E_{\text{LUMO}})$$

$$\chi = -1/2(E_{\text{HOMO}} + E_{\text{LUMO}})$$

$$\delta = 1/\eta$$

$$\omega = \chi^2/2\eta$$

2.2. Protein preparation and molecular docking

Three-dimensional crystal structure of human sex-hormone globulin

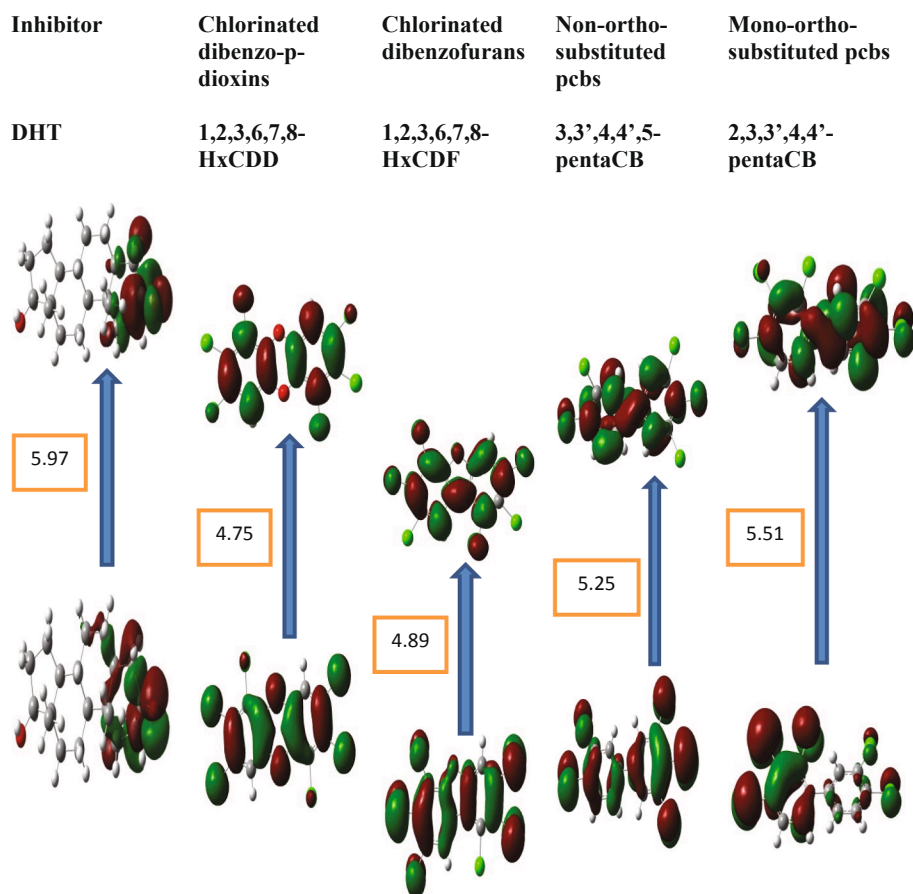


Fig. 4. The calculated ground state isodensity surface plots for Frontier molecular orbitals (FMOs) for investigated DHT and the most potent inhibitor from each DLC category.

binding (PDB ID: 1D2S) was retrieved in PDB format from online protein data bank (PDB) [31]. AutoDock 4.2.6 was used to perform the docking of DLCs with human SHBG [32]. AutoDock utilizes a semi empirical free energy force field to calculate the binding free energy of a small molecule to a macromolecule. Receptor molecule was prepared by removing heteroatoms, also by adding explicit hydrogen molecules and associated Kollman charges (16.0) by utilizing the AutoDock Tools 1.5.6 and saved in .pdbqtfile format. All hetero atoms and water molecules were eliminated and energy minimization of the protein implemented using AutoDock 4.2.6. The 3D structures of all the DLCs were drawn using Gauss View 5.0. The ligands were prepared by adding hydrogen atoms and Gasteiger charges and then saved in .pdbqt format. Ligand flexibility was used to specify the torsional degrees of freedom in ligand molecule. For docking purpose, Lamarckian genetic algorithm and grid supported energy evaluation method were adopted. The pose with the maximum binding affinity score and the corresponding interactions was selected and further visually inspected and analyzed in LigPlot.

2.3. Molecular dynamics simulation

The associated structural and dynamic changes occurring at the atomistic level in hSHBG on the binding of DLCs were analysed by molecular dynamics simulation. The simulation study was performed with Gromacs 5.1.1 suite with GROMOS96 43a1 force field [33,34]. DHT and DLCs topology files were generated using Prodrug server. The protein complexes were solvated in a cubic box with simple point charge (SPC) waters and counter ions were added for the overall electrostatic neutrality of the system. Energy minimization was performed to minimize the steric clashes by using Steepest descent algorithm for 50,000 iteration steps and cut-off up to 1000 kJmol^{-1} . Then the system was

equilibrated in two different phases for 50,000 steps. The first phase of equilibration was done with a constant number of particles, volume, and temperature (NVT), each step 2 fs. The second phase of equilibration was performed with a constant number of particles, pressure, and temperature (NPT), the ensemble at 300 K.

The final production step of molecular dynamics simulation was carried out for 20 ns, each step of 2 fs. Trajectories were saved and results were analyzed using XMGRACE. Root mean square deviation (RMSD) variation in protein backbone was calculated by using g rms tool which utilizes the least-square fitting method. Overall root mean square fluctuation (RMSF) in the atomic positions of protein $\text{C}\alpha$ backbone was calculated by using the g rmsf tool. A rough measure of compactness factor of protein during the course of the simulation was estimated by using the g gyrate tool of GROMACS. gmX sasa was used for computation of the total solvent accessible surface area (SASA). Hydrogen bonds were calculated with 3.5 \AA distance cut-off by using g hbond and the distribution of intermolecular hydrogen bond lengths throughout the simulation were also analyzed.

3. Results and discussion

3.1. DFT calculation studies

The theoretical DFT calculations were performed in gas phase by DFT method at B3LYP 3-21G basis set. All optimum DLCs are stable, and this is approved in terms of the absence of the imaginary frequency. The results of the theoretical DFT calculations for all investigated DLCs revealed the planarity.

Table 2Free energy (in Hartree), dipole moment (Debye), polarizability (Bohr³) and TEF of all ligands.

DLCs/ Ligand category	DLC/ Ligand	Free energy	Dipole moment	Polarizability (α)	WHO-TEF	
Inhibitor	DHT	-887.69	2.66	180.69	-	
Chlorinated dibenzo-p-dioxins	2,3,7,8-TCDD	-2438.71	0.00	169.79	1	
	1,2,3,7,8-PeCDD	-2896.09	1.43	180.34	1	
	1,2,3,4,7,8-HxCDD	-3353.48	0.31	191.44	0.1	
	1,2,3,6,7,8-HxCDD	-3353.48	0.00	191.06	0.1	
	1,2,3,7,8,9-HxCDD	-3353.48	2.70	190.41	0.1	
	1,2,3,4,6,7,8-HpCDD	-3810.86	1.28	201.67	0.01	
	OCDD	-4268.24	0.00	212.40	0.0003	
	Chlorinated dibenzofurans	2,3,7,8-TCDF	-2363.92	0.75	167.96	0.1
		1,2,3,7,8-PeCDF	-2821.30	0.90	179.49	0.03
		2,3,4,7,8-PeCDF	-2821.31	2.09	177.63	0.3
1,2,3,4,7,8-HxCDF		-3278.69	0.57	189.74	0.1	
1,2,3,6,7,8-HxCDF		-3278.69	1.02	189.27	0.1	
1,2,3,7,8,9-HxCDF		-3278.69	2.14	190.60	0.1	
2,3,4,6,7,8-HxCDF		-3278.68	3.06	188.06	0.1	
1,2,3,4,6,7,8-HpCDF		-3736.06	1.61	200.01	0.01	
1,2,3,4,7,8,9-HpCDF		-3736.07	0.91	200.95	0.01	
OCDF		-4193.44	0.19	211.47	0.0003	
Non-ortho-substituted PCBs	3,3',4,4'-tetraCB	-2290.32	1.25	160.22	0.0001	
	3,4,4',5-tetraCB	-2290.31	1.85	164.97	0.0003	
	3,3',4,4',5-pentaCB	-2747.71	1.84	171.82	0.1	
	3,3',4,4',5,5'-hexaCB	-3205.09	0.00	188.13	0.03	
Mono-ortho-substituted PCBs	2,3,3',4,4'-pentaCB	-2747.70	3.83	166.45	0.00003	
	2,3,4,4',5-pentaCB	-2747.70	1.39	167.97	0.00003	
	2,3',4,4',5-pentaCB	-2747.71	1.73	168.34	0.00003	
	2',3,4,4',5-pentaCB	-2747.71	2.87	167.95	0.00003	
	2,3,3',4,4',5-hexaCB	-3205.07	2.42	187.37	0.00003	
	2,3,3',4,4',5'-hexaCB	-3205.09	3.03	178.39	0.00003	
	2,3',4,4',5,5'-hexaCB	-3205.09	1.56	180.00	0.00003	
	2,3,3',4,4',5,5'-heptaCB	-3662.47	1.24	190.51	0.00003	

3.1.1. Frontier molecular orbitals

Molecular orbitals (MO) energies were calculated to estimate the reactivities of the DLCs. More specifically, the MO energies of the highest occupied molecular orbital (HOMO) and the lowest unoccupied molecular orbital (LUMO) were calculated, and from those the gap in energy between the HOMO and the LUMO energies (GAP) was calculated. According to calculated MO energies, PCDFs are the strongest electron acceptors, i.e., they have the lowest LUMO energies, among the DLCs. Moreover, PCDFs and PCBs are stronger electron donors, i.e., they have lower HOMO energies, than PCDDs. PCBs are the most stable chemical class among the DLCs based on their higher GAP values compared to the other DLCs. This high chemical class dependence suggests that the MO energies are not sufficient to explain the congener-specific differences seen in biological activity among DLCs. Because of this, we instead focused on the reactivity descriptors of the DLCs. Moreover, HOMO and LUMO are very important quantum chemical parameters to determine the reactivity of the molecules and are used to calculate many important parameters such as the chemical reactivity descriptors. The energies of the HOMOs and LUMOs of the studied DLCs were calculated using DFT method at B3LYP 3-21G basis set and are tabulated in Table 1. The isodensity surface plots of HOMO and LUMO for DHT and the most potent inhibitor from each DLC category are shown in Fig. 4.

3.1.2. Thermodynamic parameters

The spontaneity of a chemical reaction and the stability of the reaction product can be predicted from thermodynamic properties such as Gibbs' free energy. Free energy is a pivotal criterion to represent the interactions of binding partners where both the sign and magnitude are important to express the likelihood of bimolecular events occurring. Greater negative values indicate improved thermodynamic properties. In this study, it is found that the values are negative (Table 2) meaning the binding will occur spontaneously without any extra energy expenditure. Free energy of DHT is -887.69 Hartree whereas DLCs shows the high values which suggesting that the molecules are energetically and configurationally preferable. The dipole moment of DHT is 2.66 Debye

whereas DLCs shows the high dipole moment. Elevated level of dipole moment enhances the nonbonding interaction, binding affinity and polar nature of a molecule.

The DFT estimated data revealed that the high dipole moment PCDFs and PCBs could illustrate their binding pose within a specific target protein and their results of the predicted binding affinity that will be discussed in the following molecular docking part. The polarizability of the materials depends on how the susceptibility of molecular system electron cloud be affected by approaching of a charge. Moreover, it depends on the complexity of the compounds as well as the size of the molecular structure. Molecules of the large size are more polarizable compounds. It is worth noting that the more chlorinated DLCs of the highest complexity is predicted to have the highest polarizability.

3.1.3. Molecular orbital properties

Recently, many reports showed that the FMOs have to be taken into consideration in investigation of the structure activity relationships. The FMOs theory showed that the energy level of the HOMO and the LUMO are the most significant aspects that impact the bioactivities of small structural ligands. Obviously, the level of energy of HOMOs are different for all investigated DLCs. Chemical hardness (η) and softness (δ) of a molecule can be determined from the HOMO (highest occupied molecular orbital) - LUMO (lowest unoccupied molecular orbital) gap. Large HOMO-LUMO gap related to high kinetic stability and low chemical reactivity and small HOMO-LUMO gap is important for low chemical stability, because addition of electrons to a high-lying LUMO and/ or removal of electrons from a low-lying HOMO is energetically favorable in any potential reaction.

3.1.4. Molecular electrostatic potential (MEP)

To validate the evidence about the reactivity of the DLCs as inhibitors, the molecular electrostatic potential (MEP) is important to be calculated. Although the MEP gives an indication about the molecular size and shape of the positive, negative as well as the neutral electrostatic potential. These could be a tool to predict physicochemical property relationships with the molecular structure of the DLCs under

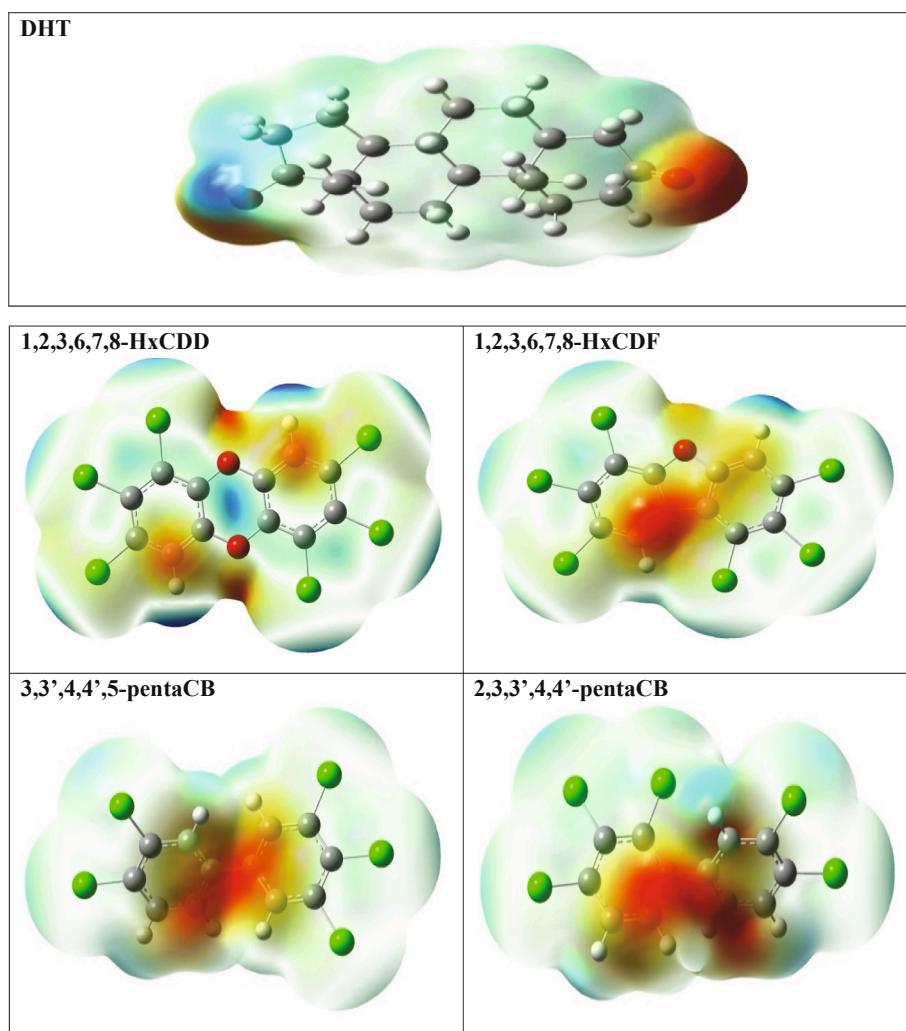


Fig. 5. Molecular electrostatic potentials (MEP) of DHT and the most potent inhibitor from each DLC category.

Table 3

The Mulliken atomic charges of DHT and the most potent inhibitor from each DLC category.

Inhibitor	Chlorinated dibenzo-p-dioxins		Chlorinated dibenzofurans		Non-ortho-substituted pcbs		Mono-ortho-substituted pcbs		
DHT	1,2,3,6,7,8-HxCDD		1,2,3,6,7,8-HxCDF		3,3',4,4',5-pentaCB		2,3,3',4,4'-pentaCB		
1 O	-0.221239	1 C	0.378893	1 C	0.374042	1 C	0.097947	1 C	0.095946
2 O	-0.455606	2 C	0.32407	2 C	0.033733	2 C	0.03344	2 C	0.063687
3 C	-0.039167	3 C	0.100019	3 C	0.095604	3 C	-0.005556	3 C	0.018984
4 C	0.036809	4 C	-0.265791	4 C	-0.258903	4 C	0.092817	4 C	-0.271061
5 C	0.043073	5 C	-0.268516	5 C	-0.264412	5 C	-0.261489	5 C	-0.250752
6 C	-0.123429	6 C	-0.313828	6 C	-0.311851	6 C 10 C	-0.265649	6 C	-0.25245
7 C	-0.10309	8 C	-0.265779	7 C	-0.25853	11 C	0.095446	9 C	0.041787
8 C	0.000965	9 C	-0.268515	8 C	-0.261606	12 C	-0.251257	10 C	0.093973
9 C	0.008382	10 C	-0.313848	9 C	-0.301685	13 C	-0.258291	11 C	-0.263466
10 C	0.036047	11 C	0.378919	10 C	0.055457	14 C	-0.251594	12 C	-0.262177
11 C	0.015216	12 C	0.324074	11 C	0.330238	15 C	0.096783	13 C	0.119802
12 C	-0.000376	13 C	0.100012	12 C	0.095432	18 Cl	-0.00164	14 C	-0.024967
13 C	0.284038	14 O	-0.579326	14 O	-0.548619	19 Cl	0.164108	17 Cl	0.169397
14 C	0.017592	15 O	-0.579326	15 Cl	0.222356	20 Cl	0.215403	18 Cl	0.159703
15 C	-0.017637	16 Cl	0.221782	16 Cl	0.171873	21 Cl	0.168091	19 Cl	0.159407
16 C	0.068334	17 Cl	0.183231	17 Cl	0.184494	22 Cl	0.169532	20 Cl	0.210882
17 C	0.018202	18 Cl	0.183237	18 Cl	0.216394		0.161911	21 Cl	0.191306
18 C	0.039566	19 Cl	0.221773	19 Cl	0.223316				
19 C	-0.002476	20 Cl	0.219463	20 Cl	0.202667				
20 C	-0.042749	21 Cl	0.219456						
21 C	0.437545								

Table 4

Details of molecular docking results: the summary of binding affinities (kcal/mol) and the hydrophobic interactions of the DLCs-SHBG complexes.

DLCs/ Ligand category	DLC/ Ligand	Binding energy (kcal/mol)	Interacting residues	Common residues	
Inhibitor	DHT	-10.94	Thr40, Phe56, Leu171, Ser42, Gly58, Val105, Ile141, Phe67, Trp66, Asp59, Asn82 (2.85 Å), Asp65(2.81 Å)	100%	
Chlorinated dibenzo-p-dioxins	2,3,7,8-TCDD	-7.19	Thr60, Leu34, Gly58, Phe67, Asn82, Asp65, Leu80, Met139, Gly129, His136, Trp84	33%	
	1,2,3,7,8-PeCDD	-7.60	Phe56, Ser42, Val105, Ile141, Phe67, Trp66, Asn82, Val127, Leu80, Ser128, Met107, Lys106, Ser41, Val112	58%	
	1,2,3,4,7,8-HxCDD	-7.20	Phe67, Leu80, Met139, Trp84, Ser128, Val112, Met107, Leu171	17%	
	1,2,3,6,7,8-HxCDD	-8.04	Leu80, Gly58, Phe67, Asn82, Trp66, Phe56, Ile141, Leu171, Ser42, Ser41, Lys106, Val105, Val112, Val127	75%	
	1,2,3,7,8,9-HxCDD	-7.19	Trp66, Phe148, Lys63, His81, Pro62, Asn152	8%	
	1,2,3,4,6,7,8-HpCDD	-7.42	Leu34, Phe67, Asn82, Leu80, Met139, Trp84, Ser128, Leu171, Met107, Val112	25%	
	OCDD	-7.67	Leu34, Phe67, Asn82, Leu80, Met139, Trp84, Ser128, Leu171, Met107, Val112, Val105	33%	
	Chlorinated dibenzofurans	2,3,7,8-TCDF	-7.84	Phe56, Leu171, Ser42, Val105, Ile141, Phe67, Asp59, Asn82, Asp65	75%
		1,2,3,7,8-PeCDF	-8.48	Phe67, Asn82, Leu80, Trp66, Ser42, Leu171, Val105, Ile141, Phe56, Gly58, Asp59, Asp65	92%
		2,3,4,7,8-PeCDF	-8.46	Phe67, Asn82, Leu80, Ser42, Leu171, Val105, Ile141, Phe56, Met107, Val112	58%
1,2,3,4,7,8-HxCDF		-8.63	Phe67, Asn82, Leu80, Ser42, Val105, Ile141, Phe56, Gly58, Asp59, Asp65, Met139, Val112	75%	
1,2,3,6,7,8-HxCDF		-9.12	Phe67, Asn82, Leu80, Ser42, Val105, Ile141, Phe56, Gly58, Asp59, Asp65, Val112, Trp66, Leu171	92%	
1,2,3,7,8,9-HxCDF		-8.81	Phe67, Asn82, Ser42, Ser41, Val105, Ile141, Phe56, Gly58, Asp59, Asp65, Val112, Trp66, Leu171, Met107, Lys106	92%	
2,3,4,6,7,8-HxCDF		-8.04	Thr40, Phe56, Ser41, Gly58, Val105, Ile141, Phe67, Asp65, Met107, Ser128	58%	
1,2,3,4,6,7,8-HpCDF		-8.52	Asn82, Ser41, Val105, Ile141, Gly58, Asp59, Asp65, Val112, Trp66, Leu171, Met107, Lys106, Leu80, Met139, Thr40	75%	
1,2,3,4,7,8,9-HpCDF		-8.82	Asn82, Ser41, Ser42, Val105, Ile141, Gly58, Asp59, Asp65, Val112, Leu171, Met107, Lys106, Met139, Phe56, Ser128	75%	
OCDF		-7.61	Leu34, Met139, Met107, Leu171, Val105, Val112, Phe67, Trp84, Ser128	25%	
Non-ortho-substituted PCBs	3,3',4,4'-tetraCB	-8.38	Asn82, Phe67, Asp59, Asp65, Phe56, Val105, Ser42, Lys106, Val112, Trp66	67%	
	3,4,4',5'-tetraCB	-7.92	Asn82, Phe67, Asp59, Asp65, Phe56, Val105, Ser42, Trp66, Gly58, Ser41, Leu80	75%	
	3,3',4,4',5'-pentaCB	-8.43	Asn82, Phe67, Asp59, Asp65, Phe56, Val105, Ser42, Trp66, Gly58, Met107, Lys106, Val112, Ile141	83%	
Mono-ortho-substituted PCBs	3,3',4,4',5,5'-hexaCB	-7.96	Asn82, Phe67, Asp59, Asp65, Val105, Ser41, Ser42, Trp66, Gly58, Met107, Lys106, Val112, Ile141, Leu171, Leu80	83%	
	2,3,3',4,4',5-pentaCB	-8.96	Asn82, Phe67, Asp59, Asp65, Ser41, Trp66, Gly58, Met107, Ile141, Leu80, Phe56, Thr40	75%	
	2,3,4,4',5-pentaCB	-8.60	Asn82, Phe67, Asp59, Asp65, Ser41, Trp66, Gly58, Leu80, Phe56, Met139, Val105, Ser42	75%	
	2,3',4,4',5-pentaCB	-8.84	Asn82, Phe67, Asp59, Asp65, Trp66, Gly58, Phe56, Val105, Ser42, Thr60, Ile141, Lys106	83%	
	2',3,4,4',5-pentaCB	-8.56	Asn82, Phe67, Asp59, Asp65, Trp66, Gly58, Phe56, Val105, Ser42, Ser41, Leu80	75%	
	2,3,3',4,4',5-hexaCB	-8.71	Asn82, Phe67, Asp59, Asp65, Trp66, Gly58, Phe56, Ser42, Leu80, Met139, Val105, Thr40	83%	
	2,3,3',4,4',5'-hexaCB	-8.36	Asn82, Phe67, Asp59, Asp65, Trp66, Phe56, Ser41, Ser42, Leu80, Met139, Val105, Lys106, Met107, Ile141	75%	
	2,3',4,4',5,5'-hexaCB	-8.90	Asn82, Phe67, Asp59, Asp65, Phe56, Ser41, Ser42, Leu80, Val105, Lys106, Met107, Gly58, Thr40	75%	
	2,3,3',4,4',5,5'-heptaCB	-7.97	Asn82, Phe67, Asp59, Asp65, Phe56, Ser41, Leu80, Met107, Gly58, Thr40, Trp66, Met139, Leu171	75%	

investigation [33]. Moreover, the molecular electrostatic potential is a useful tool to estimate the reactivity of the DLCs toward electrophilic and nucleophilic attacks. The molecular electrostatic potential of the known inhibitor, DHT and the most potent inhibitor from each DLC category were calculated by the same method under the same base sets and seen in Fig. 5.

In the MEP, the maximum negative region is the preferred sites for electrophilic attack, indicated as red color. So, an attacking electrophile will be attracted by the negatively charged sites, and the opposite situation for the blue regions. It is obvious that the molecular size and the shape as well as the orientation of the negative, positive, and the neutral electrostatic potential varied according to the compound because of the type of the atoms and its electronic nature. The difference in the mapping of the electrostatic potential around the DLCs could be principally responsible for variation of its binding affinity with the active sites receptor.

3.1.5. Mulliken atomic charges

The Mulliken atomic charges of the estimated ligands were

calculated with DFT using B3LYP 3 as a method at -21G at a basis set, the data were tabulated in Table 3. It showed that the C21 is the most positive and O2 have the most negative charge for DHT. On the other hand, it is observed that the most nucleophilic centers of 1,2,3,6,7,8-HxCDD are O14 and O15 which are the most electrophilic susceptibility positions. However, 14O, 6C and 4C are the most negative charges of 1,2,3,6,7,8-HxCDF, 3,3',4,4',5-pentaCB and 2,3,3',4,4'-pentaCB and their respective positively charged atoms are 1C, 19Cl and 20Cl. The positively charged centers are the most susceptible sites for nucleophilic attacks i.e., electron donation. However, the most negatively charged centers are the most susceptible sites for electrophilic one.

3.2. Molecular docking

In order to characterize the molecular interactions, molecular docking of co-crystallized substrate analogue, dihydrotestosterone (DHT) along with DLCs was performed within the binding pocket of human SHBG using AutoDock 4.2.6. All the generated binding poses were ranked and clustered according to their binding affinity. The

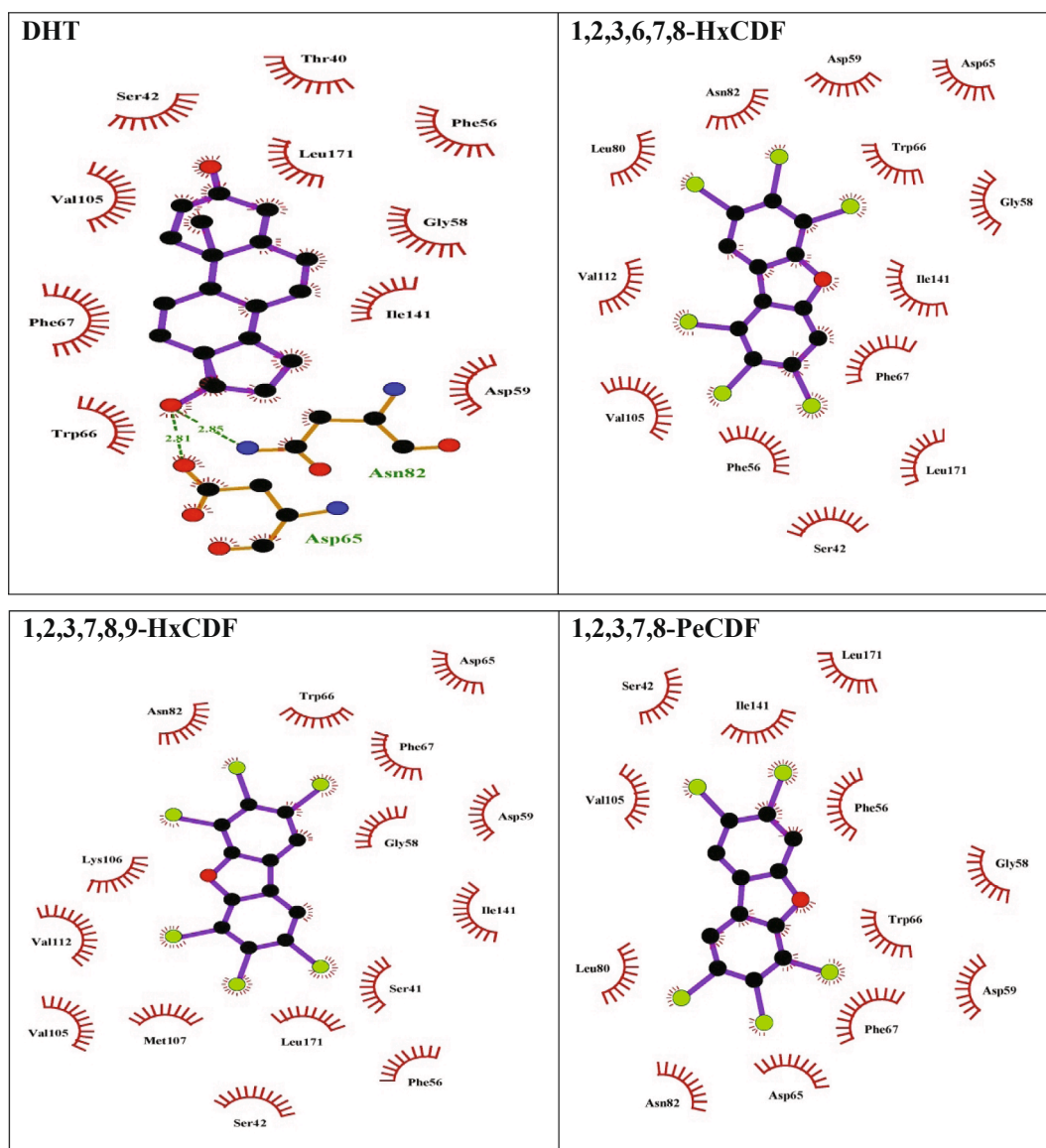


Fig. 6. Molecular interaction of selected DLCs and DHT (green dots represent H-bond) with hSHBG. The interacting residues of hSHBG are represented in red semi-circle form. (For interpretation of the references to color in this figure legend, the reader is referred to the web version of this article.)

AutoDock results show that the binding affinity ranged from -7.19 to -8.04 kcal/mol for PCDDs; -7.61 to -9.12 kcal/mol for PCDFs; -7.92 to -8.96 for PCBs which is comparable to a substrate analogue, DHT (-10.94 kcal/mol) as shown in Table 4. Mostly, all the DLCs have shown interaction with the key amino acid residues such as Ser42, Asp65, Asn82, similar to substrate analogue, DHT as shown in Fig. 6 (Green dotted lines show hydrogen bonding). This study shows that out of all the DLCs; 1,2,3,6,7,8-HxCDF, 1,2,3,7,8,9-HxCDF and 1,2,3,7,8-PeCDF were able to engage 92% of the important interacting residues of hSHBG during molecular interactions.

Dihydrotestosterone (DHT), a known ligand of SHBG, showed the lowest binding affinity, i.e., -10.94 kcal/mol and interacted hydrophobically with residues Thr 40, Phe 56, Leu 171, Ser 42, Gly 58, Val 105, Ile 141, Phe 67, Trp 66 and Asp 59. The polar interactions were found to be with Asn 82 (2.85 Å) and Asp 65 (2.81 Å). The binding affinity of DHT was attributed to the presence of hydrogen bonds along with different hydrophobic interactions between the inhibitor and the critical amino acids residues of the receptor. The result of the docking studies showed that the residue Phe 67, Asn 82, Leu 80, Ser 42, Val 105, Ile 141, Phe 56, Gly 58, Asp 59, Asp 65, Val 112, Trp 66, Leu 171

interacted hydrophobically with the 1,2,3,6,7,8-HxCDF molecule. The compound 1,2,3,7,8,9-HxCDF also shows good interaction with enzyme SHBG. Hydrophobic interactions were found with residue Phe 67, Asn 82, Ser 42, Ser 41, Val 105, Ile 141, Phe 56, Gly 58, Asp 59, Asp 65, Val 112, Trp 66, Leu 171, Met 107 and Lys 106. However, 1,2,3,7,8-PeCDF interacts hydrophobically with Phe 67, Asn 82, Leu 80, Trp 66, Ser 42, Leu 171, Val 105, Ile 141, Phe 56, Gly 58, Asp 59 and Asp65 residues. Hence, these DLCs can potentially displace or compete with the natural hSHBG ligands such as dihydrotestosterone, testosterone, and estradiol for the availability of hSHBG binding sites resulting in altered androgen-estrogen homeostasis.

4. Molecular simulation results

Molecular dynamics simulation studies provide suitable means to understand the changes occurring at the atomistic level in the protein–ligand system and emphasizes on the stability of the complex. Therefore, a simulation study was performed in order to understand the dynamics involved during binding of DLCs to hSHBG. In the present study, different parameters such as RMSD, RMSF, radius of gyration

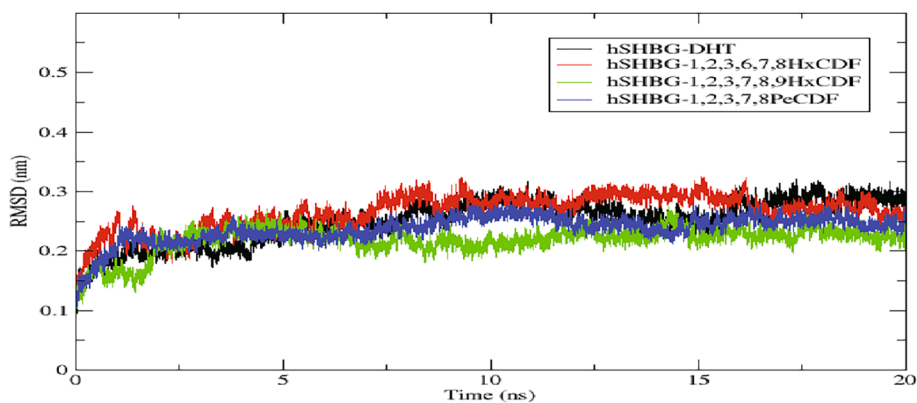


Fig. 7. RMSD profile of the $C\alpha$ backbone of hSHBG during the 20 ns of simulation at 300 K with DHT and DLCs.

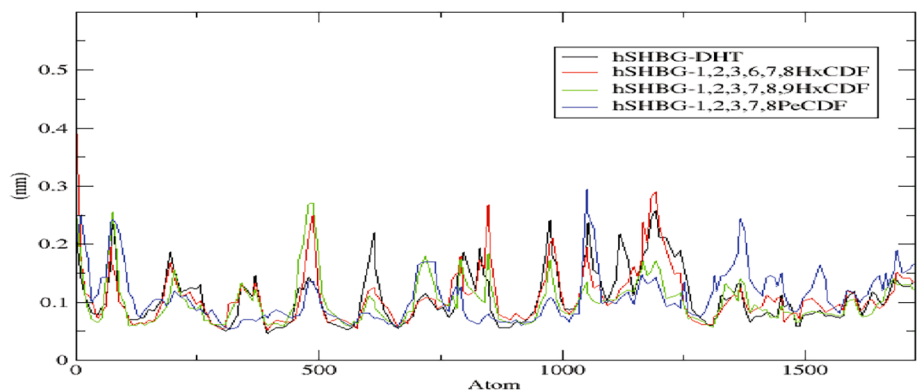


Fig. 8. RMSF molecular dynamics simulation results of hSHBG for 20 ns with DLCs and DHT.

(Rg), solvent accessible surface area (SASA) and the hydrogen bond formation and length distribution during the course of the simulation have been studied.

4.1. Root-mean-square deviation (RMSD)

It represents the dynamic stability of the protein and predicts the conformation changes occurring in the protein backbone during the simulation. Here, in the present study, RMSD values of DHT-hSHBG and DLCs-hSHBG complexes were analyzed. RMSD plots show that most of the system acquires equilibrium around 15 ns during the course of the simulation and were stable up to 20 ns as shown in Fig. 7. The high fluctuation of the RMSD values for all the complexes lies within in the

range of 2 Å to 3 Å. The RMSD results analysis implies that the binding of DLCs at the catalytic site of hSHBG is stable and does not vary the protein backbone stability.

4.2. Root-mean-square fluctuation (RMSF)

RMSF determines the flexibility of the polypeptide chain after fitting it to a reference frame. It is the fluctuation of $C\alpha$ atom coordinates from their average position during the simulation. Generally, in proteins loosely organized loops are characterized by high RMSF values while secondary structural elements show less flexibility. In the present context, atom mobility was calculated for each of the DLCs-hSHBG complexes and was plotted against the atom based on the trajectory of

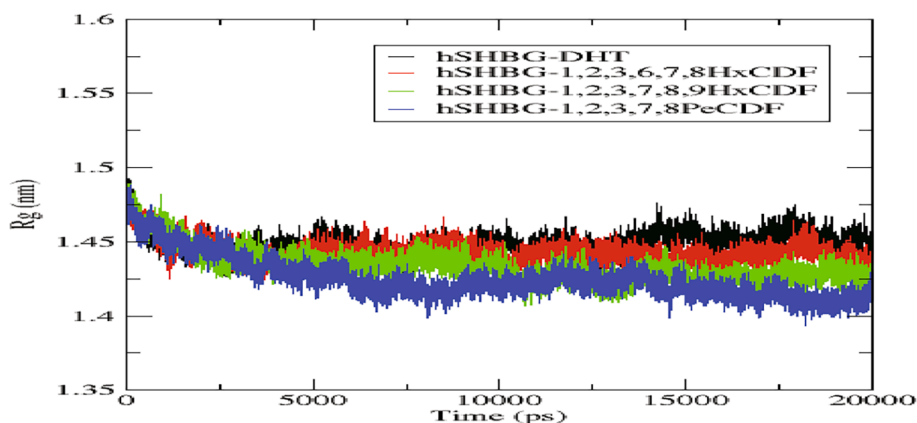


Fig. 9. Radius of gyration (Rg) plots of DHT-hSHBG and DLCs-hSHBG. The radius of gyration results associated with the compactness of the hSHBG protein for the simulation of 20 ns with DHT and DLCs.

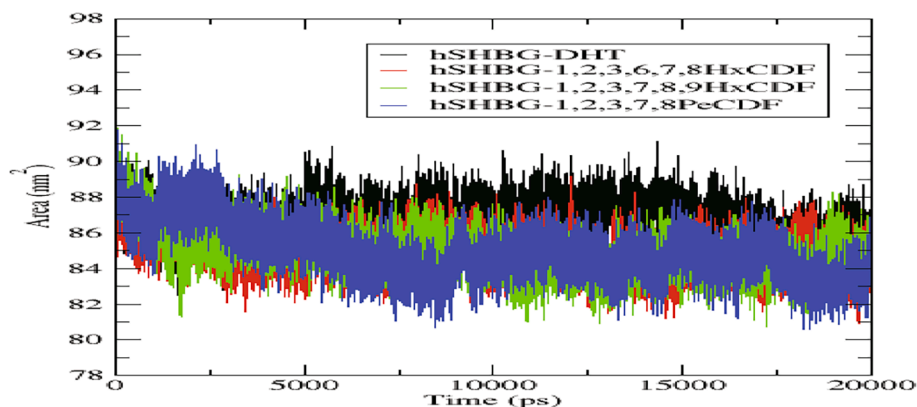


Fig. 10. Solvent accessible surface area profile of hSHBG with DHT and DLCs. SASA results of hSHBG-DHT and hSHBG-DLCs complexes during the simulation of 20 ns.

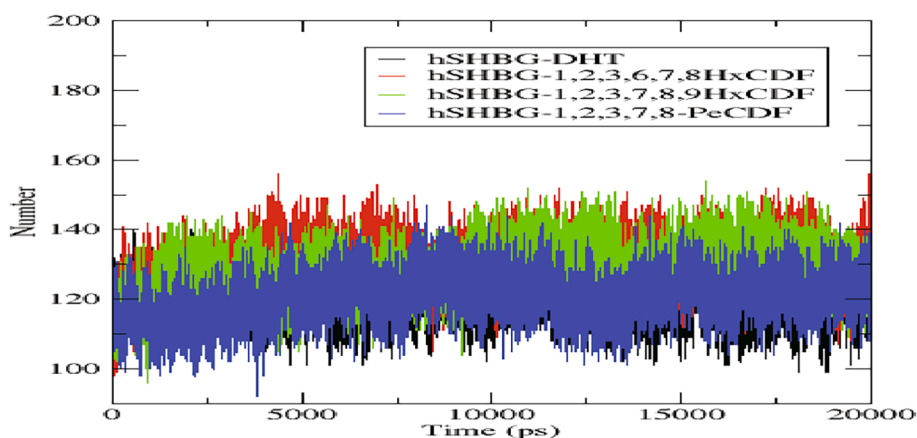


Fig. 11. Hydrogen bond number results of DHT-hSHBG and DLCs-hSHBG complexes during the 20 ns of simulation.

MD simulation, shown in Fig. 8. These results suggest that active site residues were not considerably perturbed upon binding of the ligands. Results illustrate that the RMSF fluctuation profiles of DLCs-hSHBG complexes were almost similar to DHT-hSHBG complex. Thus, the DLCs form stable complexes with hSHBG and can inhibit this important enzyme.

4.3. Radius of gyration (Rg)

Radius of gyration (Rg) factor is associated with the compactness of protein during the molecular simulation. It is simply a measure of the distance between the center of mass of the protein atoms and its terminal in a given time step. In general, a stably folded protein tends to maintain a relatively less variation in Rg value which determines its dynamic stability. In the present study, variation occurring in Rg value is plotted against time as shown in Fig. 9. The radius of gyration results shows that compactness of DLCs-hSHBG complexes is lower compared to the DHT-hSHBG complex.

4.4. Solvent accessible surface area (SASA)

Solvation free energy of each atom in a protein is contributed by its polar and non polar residue interactions. Solvent accessible surface area (SASA) is the surface area monitored by the probe of the solvent molecule when it traces the Van der Waals surface of the receptor molecule. Mostly structural alterations are monitored in the residues forming the loop region in the vicinity of the active site cavity. In general, hydrophobic residues mostly contribute to the rise of SASA value. This is also

apparent by the raised value of the solvent accessible surface area (SASA) in that region. SASA results of DLCs-hSHBG complexes are similar to DHT-hSHBG complex as shown in Fig. 10.

4.5. Hydrogen bond analysis

Hydrogen bond interaction pattern helps in maintaining the stable conformation of a protein. Hydrogen bond trajectory analysis of DHT-hSHBG and DLCs-hSHBG with respect to time was analyzed to understand the relationship between flexibility and hydrogen bond formation. DLCs-hSHBG showed comparable number of hydrogen bonds formation during the entire simulation of 20 ns compared to the DHT-hSHBG (Fig. 11). The g hbond utility of GROMACS was employed to compute the hydrogen bond numbers and distribution profiles of the complexes. The hydrogen bond results help in understanding the functionality and ability of these harmful dioxin-like compounds to efficiently hinder the activity hSHBG.

5. Conclusion

Sex hormone-binding globulin (SHBG) is a high molecular weight plasma protein that binds androgens and estrogens and plays a key role in maintaining the balance between unbound and bound sex steroids. Owing to the high ligand-binding affinity, SHBG acts as a major carrier protein for steroids in the blood, and any changes in SHBG levels effects the distribution and access of these molecules to target tissues. Dioxin-like compounds have been investigated as inhibitors for hSHBG by DFT, molecular docking calculations and simulation. This study shows

that all the computational models share together with different magnitudes and conclude that the DLCs-hSHBG complexes are stable and have binding affinities similar to natural substrate analogue complex i.e. DHT-hSHBG. Displacement of the endogenous steroids from hSHBG binding sites may disrupt the androgen-estrogen homeostasis. Current study enhances our understanding of underlying molecular mechanism of potential interfering mechanisms of DLCs in steroid homeostasis of the human body.

Declaration of Competing Interest

The authors declare that they have no known competing financial interests or personal relationships that could have appeared to influence the work reported in this paper.

Acknowledgement

The authors are thankful to Central Facility for Computational Research (CFCR), University of Lucknow for providing access to computational models throughout the work.

Funding

This research received no external funding.

References

- [1] S. Manzetti, E.R. van der Spoel, D. van der Spoel, Chemical properties, environmental fate, and degradation of seven classes of pollutants, *Chem. Res. Toxicol.* 27 (2014) 713–737.
- [2] S. Manzetti, D. van der Spoel, Impact of sludge deposition on biodiversity, *Ecotoxicology* 24 (2015) 1799–1814.
- [3] W.M. Baird, L. Diamond, Metabolism and DNA binding of polycyclic aromatic hydrocarbons by human diploid fibroblasts, *Int. J. Cancer* 22 (1978) 189–195.
- [4] J. Uetrecht, Idiosyncratic drug reactions: current understanding, *Annu. Rev. Pharmacol. Toxicol.* 47 (1) (2007) 513–539.
- [5] K. Ikehata, T.G. Duzhak, N.A. Galeva, T. Ji, Y.M. Koen, R.P. Hanzlik, Protein targets of reactive metabolites of thiobenzamide in rat liver in vivo, *Chem. Res. Toxicol.* 21 (2008) 1432–1442.
- [6] M. van den Berg, L.S. Birnbaum, M. Denison, M. De Vito, W. Farland, M. Feeley, H. Fiedler, H. Hakansson, A. Hanberg, L. Haws, M. Rose, S. Safe, D. Schrenk, C. Tohyama, A. Tritscher, J. Tuomisto, M. Tysklind, N. Walker, R.E. Peterson, The World Health Organization reevaluation of human and mammalian toxic equivalency factors for dioxins and dioxin-like compounds, *Toxicol. Sci.* 93 (2006) 223–241.
- [7] M. Van den Berg, L. Birnbaum, A.T.C. Bosveld, B. Brunstrom, P. Cook, M. Feeley, J. P. Giesy, A. Hanberg, R. Hasegawa, S.W. Kennedy, et al., Toxic equivalency factors (TEFs) for PCBs, PCDDs, PCDFs for humans and wildlife, *Environ. Health Perspect.* 106 (1998) 775–792.
- [8] North Atlantic Treaty Organization/Committee on the Challenges of Modern Society. International Toxicity Equivalency Factor (I-TEF) method of risk assessment for complex mixtures of dioxins and related compounds. Report number 176, 1988.
- [9] M. van den Berg, L. Birnbaum, A.T.C. Bosveld, B. Brunstrom, P. Cook, M. Feeley, J. P. Giesy, A. Hanberg, R. Hasegawa, S.W. Kennedy, T. Kubiak, J.C. Larsen, F.X. R. Van Leeuwen, A.K.D. Liem, C. Nolt, R.E. Peterson, L. Poellinger, S. Safe, D. Schrenk, D. Tillitt, M. Tysklind, M. Younes, F. Waern, T. Zacharewsk, Toxic equivalency factors (TEFs) for PCBs, PCDDs, PCDFs for humans and wildlife, *Environ. Health Perspect.* 106 (1998) 775–792.
- [10] N. Marinkovic, D. Pasalic, G. Ferencak, B. Grskovic, A.S. Rukavina, Dioxins and human toxicity, *Arhiv Za Higijenu Rada I Toksikologiju-Archives of Industrial Hygiene and Toxicology* 61 (2010) 445–453.
- [11] H. Raunio, In silico toxicology—non testing methods, *Front. Pharmacol.* 2 (2011) 33.
- [12] K. Kosek, J. Mavri, M.S. Dolenc, S. Gobec, S. Turk, Endocrine Disruptome- an open source prediction tool for assessing endocrine disruption potential through nuclear receptor binding, *J. Chem. Inf. Model.* 54 (2014) 1254–1267.
- [13] T. Nikita, P. Anjali, K. Ashutosh, M. Anil, Computational models reveal the potential of polycyclic aromatic hydrocarbons to inhibit aromatase, an important enzyme of the steroid biosynthesis pathway, *Comput. Toxicol.* 19 (2021), 100176.
- [14] I.A. Sheikh, R.F. Turki, A.M. Abuzenadah, G.A. Damanhour, M.A. Beg, Endocrine disruption: Computational perspectives on human sex hormone-binding globulin and phthalate plasticizers, *PLoS ONE* 11 (2016), e0151444.
- [15] E. Diamanti-Kandarakis, J.P. Bourguignon, L.C. Gludice, R. Hauser, G.S. Prins, A. M. Soto, A.C. Gore, Endocrine disrupting chemicals: An endocrine society scientific statement, *Endocr. Rev.* 30 (2009) 293–342.
- [16] G.L. Hammond, Diverse roles for sex hormone-binding globulin in reproduction, *Biol. Reprod.* 85 (2011) 431–441.
- [17] H. Dechaud, C. Ravard, F. Claustrat, A.B. de la Perriere, M. Pugeat, Xenooestrogen interaction with human sex hormone-binding globulin (hSHBG), *Steroids* 64 (1999) (1999) 328–334.
- [18] G.V. Avvakumov, A. Cherkasov, Y.A. Muller, G.L. Hammond, Structural analyses of sex hormone binding globulin reveal novel ligands and function, *Mol. Cell. Endocrinol.* 316 (2010) 13–23.
- [19] N. Kambia, A. Farce, K. Belarbi, B. Gressier, M. Luyckx, P. Chavatte, T. Dine, Docking study; PPARs interaction with the selected alternative plasticizers to di(2-ethylhexyl) phthalate, *J. Enzyme Inhib. Med. Chem.* 31 (2015) 448–455.
- [20] D.O. Carpenter, Polychlorinated biphenyls (PCBs): routes of exposure and effects on human health, *Rev. Environ. Health* 21 (2006) 1–24.
- [21] P. Grandjean, C. Gronlund, I.M. Kjaer, T.K. Jensen, N. Sorensen, A.M. Andersson, A. Juul, N.E. Skakkebaek, E. Budtz-Jorgensen, P. Weihe, Reproductive hormone profile and pubertal development in 14-year-old boys prenatally exposed to polychlorinated biphenyls, *Reprod. Toxicol.* 34 (2012) 498–503.
- [22] M.P. Gleeson, D. Gleeson, QM/MM Calculations in Drug Discovery: A Useful Method for Studying Binding Phenomena, *J. Chem. Inf. Model.* 49 (3) (2009) 670–677.
- [23] A.D. Becke, Density-functional exchange-energy approximation with correct asymptotic behaviour, *Phys. Rev. A* 38 (1988) 3098–3100.
- [24] Chengteh Lee, Weitao Yang, Robert G. Parr, Development of the Colle-Salvetti correlation-energy formula into a functional of the electron density, *Phys. Rev. B* 37 (2) (1988) 785–789.
- [25] A. Kumar, A. Pandey, A. Mishra, Computational study of novel 2,3-bis [(1-methyl-1H-imidazole-2-yl) sulfanyl] quinoxaline: Structural aspects, spectroscopic investigation, HOMO-LUMO, MESP, NLO, ADMET predictions, and molecular docking studies as potential biotin carboxylase and antibiotics resistant aminoglycoside phosphotransferase aph(2'')IVA enzyme inhibitor, *Asian J. Chem.* 32 (2020) 706–726.
- [26] H. Kruse, L. Goerigk, S. Grimme, Why the Standard B3LYP/6-31G* Model Chemistry Should Not Be Used in DFT Calculations of Molecular Thermochemistry: Understanding and Correcting the Problem, *J. Organic Chem.* 77 (2012) 10824–10834.
- [27] R. Dennington, T. Keith, J. Millam, GaussView, version 5, Semichem Inc., Shawnee Mission, KS, USA, 2009.
- [28] J.L. Calais, RG Parr and W Yang, Density-functional theory of atoms and molecules, *Int. J. Quantum Chem.* 47 (1993) 101.
- [29] R.G. Pearson, The HSAB Principle-more quantitative aspects, *Inorg. Chim. Acta* 240 (1995) 93–98.
- [30] R.G. Pearson, Absolute electronegativity and hardness correlated with molecular orbital theory, *Proc. Natl. Acad. Sci.* 83 (1986) 8440–8441.
- [31] M.J. Lucido, B.J. Orlando, A.J. Vecchio, M.G. Malkowski, Crystal structure of aspirin-acetylated human cyclooxygenase-2: insight into the formation of products with reversed stereochemistry, *Biochemistry* 55 (2016) 1226–1230.
- [32] G.M. Morris, R. Huey, W. Lindstrom, M.F. Sanner, R.K. Belew, D.S. Goodsell, A. J. Olson, AutoDock4 and AutoDockTools4. Automated docking with selective receptor flexibility, *J. Comput. Chem.* 30 (2009) 2785–2791.
- [33] D. Van Der Spoel, E. Lindahl, B. Hess, G. Groenhof, A.E. Mark, H.J. Berendsen, GROMACS: fast, flexible, and free, *J. Comput. Chem.* 26 (2005) 1701–1718.
- [34] W.F. van Gunsteren, S.R. Billeter, A.A. Eising, P.H. Hünenberger, P. Krüger, A.E. Mark, W.R. Scott, I.G. Tironi, *Biomolecular Simulation: the {GROMOS96} Manual and User Guide*, 1996.